Proceedings of the 2012 IEEE 12th International Conference on Bioinformatics & Bioengineering (BIBE), Larnaca, Cyprus, 11-13 November 2012

Prediction of the Parkinsonian subthalamic nucleus spike activity from local field potentials using nonlinear dynamic models

Kyriaki Kostoglou[1], Kostis P. Michmizos[2], Pantelis Stathis[3], Damianos Sakas[3], Konstantina S. Nikita[4] and Georgios D. Mitsis[1]

[1]Department of Electrical and Computer Engineering, University of Cyprus, Nicosia, Cyprus
[2] Department of Mechanical Engineering, Massachusetts Institute of Technology, Cambridge MA
[3] Department of Neurosurgery, National and Kapodistrian University of Athens, Athens, Greece
[4] Department of Electrical and Computer Engineering, National Technical University of Athens, Athens, Greece

Abstract - **Extracellular recordings in the area of the subthalamic nucleus (STN) of Parkinson's disease patients undergoing deep brain stimulation comprise fast events, Action Potentials and slower events, known as Local Field Potentials (LFP). The LFP is believed to represent the synchronized input into the observed area, as opposed to the spike data, which represents the output. We have shown before that there is an input-output relationship between these two components in the STN. In the present paper, we extend these observations by using LFP-driven Volterra models and the Laguerre expansion technique to estimate nonlinear dynamic models which are able to predict the recorded spiking activity. To this end, we rigorously examine the optimal model order. The improved performance of the second-order Volterra models indicates that there is a nonlinear relationship between the LFP and the spiking activity. To obtain a more compact and readily interpretable model, the most significant dynamic components of the identified Volterra models are extracted using principal dynamic mode analysis.**

Index Terms - **Nonlinear modeling, Volterra kernels, Laguerre expansion, Subthalamic nucleus, Local field potentials, Spikes, Deep brain stimulation, Extracellular recordings.**

I. Introduction

Subthalamic nucleus (STN) deep brain stimulation (DBS) is considered as the most effective surgical treatment for Parkinson's disease (PD) symptoms [1]. Extracellular recordings during DBS comprise both fast events, called Action Potentials (APs) or spikes from cells within 50-350 μm from the electrode [2] and slower events, known as Local Field Potentials (LFPs). LFPs are low-frequency potentials that reflect the synaptic activity of a population of neurons within 0.5-3 mm from the tip of the recording electrode [3]. However, phenomena unrelated to synaptic events seem to influence the LFP signal [4]. The precise relationship between LFPs and the resulting APs has been a matter of long debate. In recent studies, we have demonstrated that both the rate and timing of AP firing in the STN of Parkinsonian patients may be predicted from LFP data using microelectrode recordings [5-8]. Therefore, in the present paper we further extend the predictive relationship between LFPs acquired from the microelectrodes placed inside the STN of PD patients and the timing of the observed spiking activity. To this end, we utilized nonlinear dynamic models of the Volterra-Wiener class, which have been widely used for modeling physiological systems [9-14], including a recent successful application to the study of action potential encoding in a spider mechanoreceptor [9]. Model order selection was examined in detail, using different metrics in order to ensure that overfitting is avoided. It is shown that the employed models are able to predict accurately the timing of the spiking activity of single neurons (single-unit recordings), while the performance drops considerably for multi-unit recordings.

II. Extracellular recordings

A. Data Acquisition

Extracellular recordings were obtained from three awake, immobile and un-medicated Parkinson's disease patients undergoing bilateral DBS in the Neurosurgery Clinic at Evangelismos General Hospital, Athens, Greece [7]. No electrical stimulation was applied during the recordings. Five microelectrodes in a "Ben-gun" configuration were simultaneously advanced from the STN to the substantia nigra at steps of 1mm or less. Signals acquired near the final stimulation point inside the STN were further examined.

B. Signal Processing

In order to acquire the LFPs, the raw signals were low-pass filtered with cutoff frequency around 200 Hz. On the other hand, the spike signals were extracted by applying a high-pass filter to the raw signals with cutoff frequency around 500 Hz. The exact procedure is described elsewhere [7]. 50 Hz noise and its harmonics arising from the power supply cables were removed from the LFP by fitting 50, 100, 150 and 200 Hz sine waves to the LFP signal and subtracting the estimated components. Spike detection in the spike signal is achieved through amplitude thresholding, while superparamagnetic clustering is used for classifying spike trains according to the source neuron [15]. In this study, only recordings with single-unit or separable multi-unit activity were examined. For each source neuron observed, a binary signal was produced, indicating the absence (0) or presence (1) of a spike at a specific moment in time. Both LFP and spike signals were downsampled (fs = 1000 Hz) in order to reduce the computational complexity.

III. NONLINEAR MODELING OF STN NEURONS

A. General Discrete-Time Volterra Model

The input-output relationship of a Q-th order nonlinear, causal and dynamic system with finite memory can be expressed by the following equation in discrete time:

$$y(n) = \sum_{q=0}^{Q} \left\{ \sum_{m_1} \dots \sum_{m_q} k_q(m_1, \dots, m_q) x(n-m_1) \dots x(n-m_q) \right\}$$

where $k_q(m_1, \dots, m_q)$ are the Volterra kernels of the system. Volterra kernels can be viewed as weighting functions that describe the interaction between the input past and present values in order to generate the output signal. The zeroth-order Volterra kernel ($q=0$) is the output of the system when the input is absent. The first-order kernel ($q=1$) and the high-order kernels ($q>1$) capture the linear and nonlinear dynamics of the system respectively. An efficient way to estimate these kernels is the Laguerre expansion technique (LET), which effectively reduces the number of free parameters in the Volterra model. Using the orthonormal set of L discrete Laguerre functions (DLFs), the discretized Volterra kernels of the system can be expanded as:

$$k_q(m_1, \dots, m_q) = \sum_{j_1=0}^{L-1} \dots \sum_{j_q=0}^{L-1} c_q(j_1, \dots, j_q) b_{j_1}(m_1) \dots b_{j_q}(m_q)$$

where $b_j(m)$ denotes the jth order orthonormal DLF. The expansion coefficients $c_q(j_1, \dots, j_q)$ can be estimated using least-squares estimation based on the input and output data (LFP and the resulting spikes in binary form) [12].

B. Model training and testing

The General Discrete-time Volterra model is trained using 50% of the data points available from each recording. To avoid overfitting, the remaining 50% of the data points are used to test the model. Training involves estimating the appropriate polynomial order of the model Q, the number of DLFs L and the value of the Laguerre parameter ($0<\alpha<1$), which determines the rate of exponential asymptotic decline of the DLFs. In order to quantify the performance of the model, we used the two metrics described below:

Area Under the Curve: In order to generate a binary output, we applied various thresholds to the (continuous) Volterra model output for both the training and testing sets. Consequently, the true positive rate (TPR) and false positive rate (FPR) of the model prediction were computed according to the relations:

$$TPR = \frac{TP}{P}$$

$$FPR = \frac{FP}{N}$$

where TP is the number of correctly predicted spikes in a time window of $\pm 1ms$, FP is the number of incorrectly predicted spikes, P is the number of actual spikes and N the number of non-spike events. By plotting these two quantities for each threshold value, we obtain a corresponding receiver operating characteristic (ROC) curve. The accuracy of the model prediction can be quantified by the Area Under the Curve. An area of 1 represents excellent performance, while a performance that is close to chance corresponds to an AUC value of 0.5.

Matthews Correlation Coefficient (MCC): In order to better discriminate the differences between models with high AUC values, MCC values were calculated according to the relationship:

$$MCC = \frac{TP \cdot TN - FP \cdot FN}{\sqrt{P \cdot N \cdot P' \cdot N'}}$$

where TN is the number of correctly predicted non-spike events, FN is the number of incorrectly predicted non-spike events, P' is the number of predicted spikes and N' the number of predicted non-spike events. A MCC value of 1 corresponds to an excellent prediction, while a value of -1 indicates a total disagreement between prediction and observation. The threshold value that yielded the maximum MCC in the training set was directly applied to the testing set.

The optimal training parameters (Q, L, α) are selected by applying the cross-validation technique. The model with the maximum mean AUC and MCC value in the testing set was selected as the optimal.

C. Principal Dynamic Modes Model

In order to obtain a more compact and readily interpretable model, the most significant dynamic components of the identified Volterra model were extracted using the principal dynamic mode (PDM) analysis [12]. The purpose of the PDM method is to extract a minimum set of linear filters, termed "principal dynamic modes", which can adequately approximate the system output (Fig. 1). The PDMs of the system can be computed by creating the matrix:

$$\boldsymbol{R} = \begin{bmatrix} k_0 & \frac{1}{2}\boldsymbol{k_1^T} \\ \frac{1}{2}\boldsymbol{k_1} & \boldsymbol{k_2} \end{bmatrix}$$

where $k_0, \boldsymbol{k_1}, \boldsymbol{k_2}$ are the zeroth, first and second-order Volterra kernels respectively. The eigenvectors $\boldsymbol{\mu_i}$ that correspond to the most significant eigenvalues λ_i of $\boldsymbol{R}$ (in terms of their absolute value) define the PDMs of the system. The input signal $x(n)$ is convolved with the latter:

$$u_i(n) = \sum_{m=0}^{M} \mu_i(m) x(n-m)$$

and the resulting outputs u_i are introduced into a multi-input static nonlinearity $f(u_1, u_2, \dots u_r)$. The predicted spikes are obtained by applying a threshold (specifically, the threshold value that corresponds to the maximum MCC value in the training set) to the continuous output of the static nonlinearity:

$$\hat{y}(n) = \begin{cases} 1 \ if \ f(u_1, u_2, \dots u_r) \geq THRESHOLD \\ 0 \ if \ f(u_1, u_2, \dots u_r) < THRESHOLD \end{cases}$$

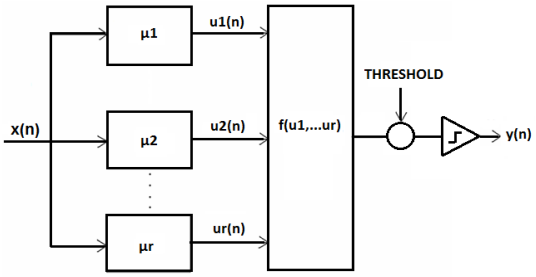

Figure 1: Principal Dynamic Modes model

The static nonlinearity $f(u_1, u_2, \dots u_r)$ was modeled by a Gaussian mixture model (GMM) fitted to the training data using the Expectation – Maximization algorithm, as it reflects the probability of AP firing for a particular PDM output values combination. An Artificial Neural Network (ANN) was also examined. The number of neurons in the input and hidden layer were equal to the number of the PDMs, while the output layer consisted of only one neuron. Hyperbolic tangent activation functions are employed both in the hidden and output layer. The ANN is trained using the Resilient Back-propagation (Rprop) method, mostly due to its speed of convergence [16].

IV. Results

First and second-order models were examined. Second-order models exhibited higher prediction accuracy for the training and testing data. On the other hand, third-order models yielded higher testing prediction errors overall, suggesting that second-order models are adequate to model the data. Thus, results from higher-order models (Q>2) are not presented hereby.

The obtained first and second-order Volterra kernels for a representative data set are given in Figs. 2 and 3 respectively. The effective memory of both kernels was around 10 ms (the time axis extends in the past).

As pre-mentioned, the first-order kernel describes the linear effects of the input on the output at various time lags. For negative-valued inputs preceded by positive-valued inputs, the first-order kernel denoted a facilitatory effect on the output of the model (Fig. 2).

The diagonal values of the second-order kernel (Fig. 3) reflect the influence of the squared value of the input on the output at each time lag, whereas the off-diagonal values represent interactions between two input values at different time lags.

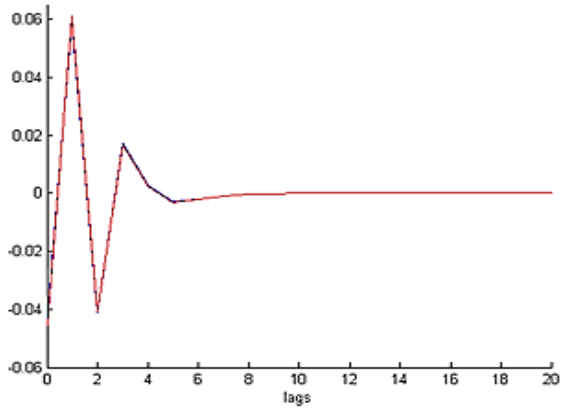

Figure 2: First-order Volterra kernel

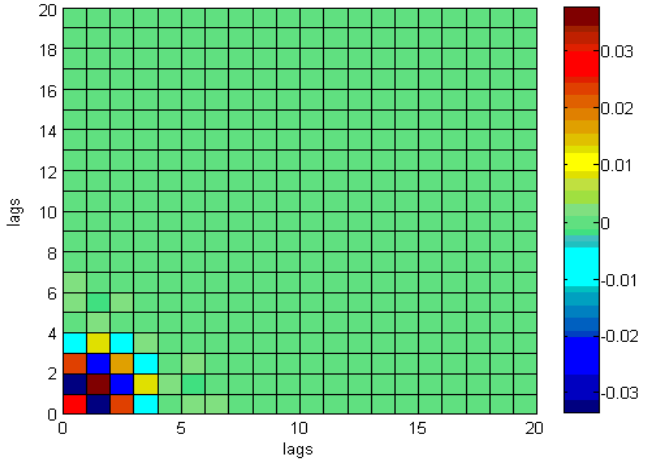

Figure 3: Second-order Volterra kernel

Two PDMs were extracted from the identified Volterra model (Fig. 4). The most significant PDM (PDM1) exhibits high frequency characteristics and it resembles the first-order kernel in the time domain (Fig. 2). Since the LFP and the PDMs are sampled every 1ms (fs = 1000 Hz) and the LFP is a low frequency signal, the only fast events that can evoke excitatory behavior on the output are the transient changes in the LFP sign (Fig. 5) that consistently precede spikes. In turn, this gives rise to the first PDM high frequency characteristic (over 200 Hz).

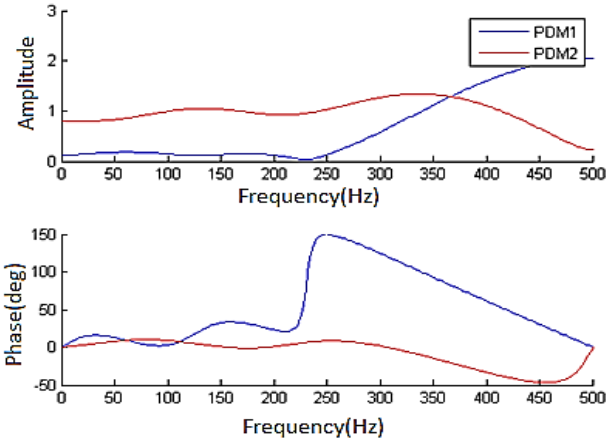

Figure 4: PDMs in frequency domain

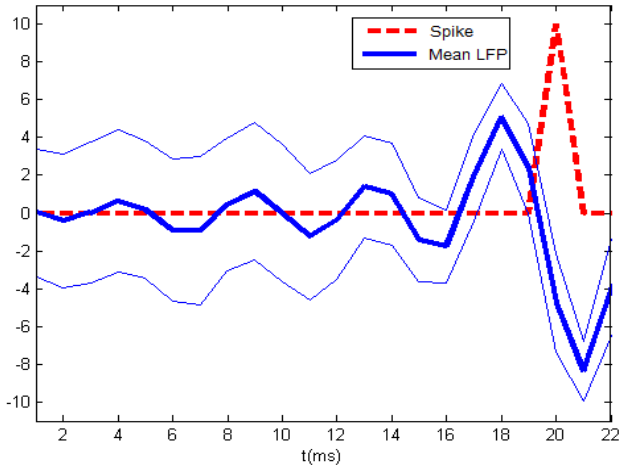

Figure 5: Mean LFP 20ms before a spike

The PDM outputs $u_1(n)$ and $u_2(n)$ were obtained by convolving the input signal with the first and second PDM respectively. Fig. 6 illustrates the values of u_1 and u_2 that correspond to spikes and non-spike events.

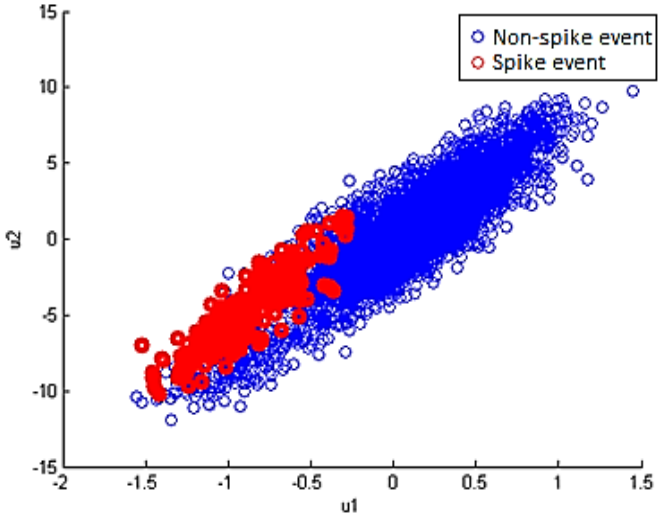

Figure 6: Scatter plot of the PDM output values that correspond to non-spike (blue) and spike (red) events

After training the GMM (based on the values of u_1 and u_2 that respond to spikes) and the ANN (based on the values of u_1 and u_2 that respond both to spike and non-spike events), we obtained an estimate of the static nonlinearity (probability of firing function) [9] (Figs. 7 and 8), which corresponds to the probability that a combination of the PDM output values will give rise to a spike. The ANN and GMM predicted spikes are shown in Fig. 9 and Fig. 10. The prediction accuracy for this particular recording was high. The ANN predicted 113 out of a total of 137 spikes in the testing set and mispredicted only 17 out of 3189 non-spike events (Fig. 9). The GMM predicted correctly 117 spikes but it exhibited a higher false positive rate compared to the ANN (Fig. 10).

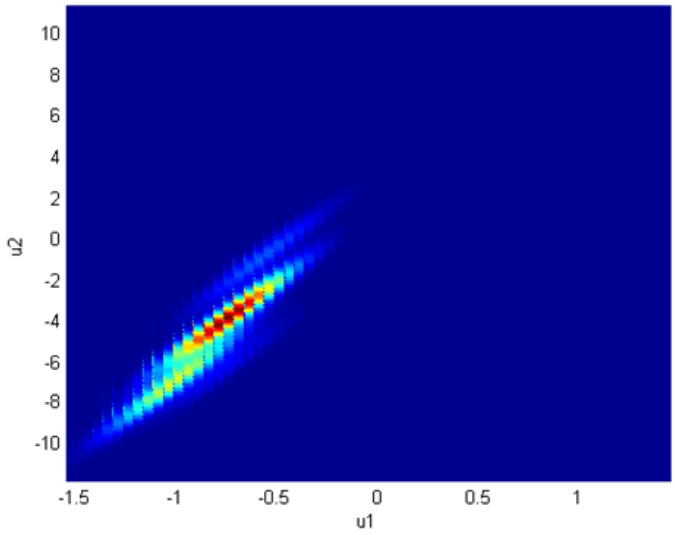

Figure 7: Probability of firing based on the GMM

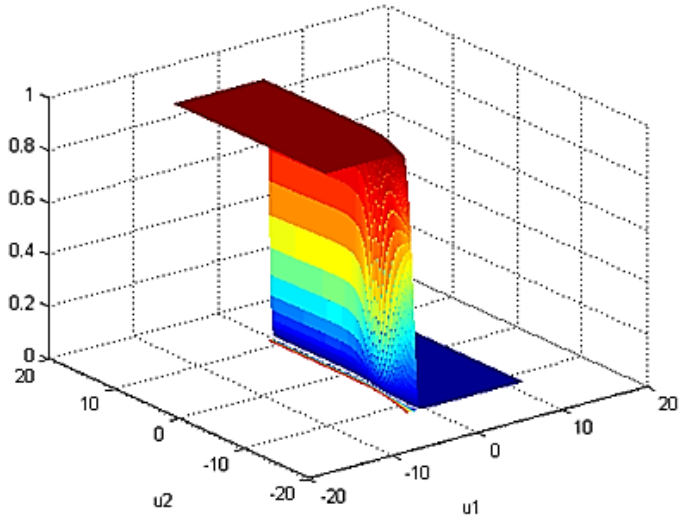

Figure 8: Probability of firing based on the ANN

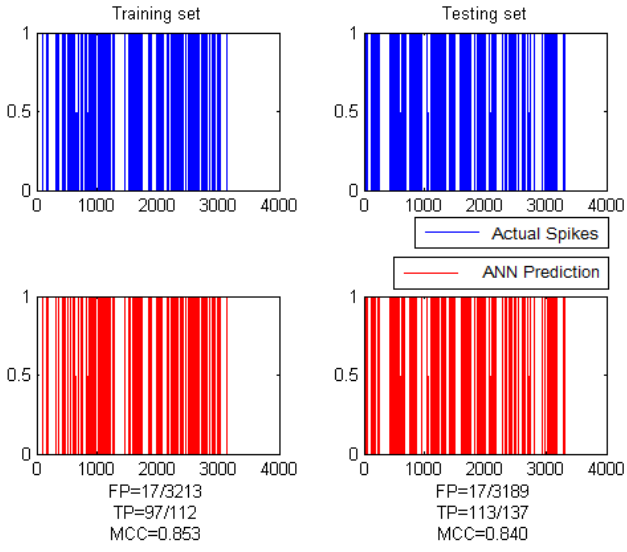

Figure 9: ANN spike predictions for the training and testing set

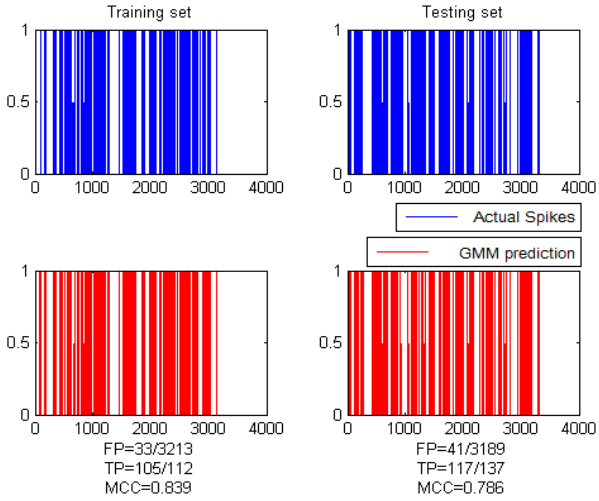

Figure 10: GMM spike predictions for the training and testing set

V. Discussion and Conclusions

Volterra kernels have been proven as an efficient tool for modeling the LFP-spike timing relationship. The improved performance of the second-order Volterra models indicated that there is a nonlinear relationship between these two quantities. The PDMs extracted from the Volterra kernels correspond to the most significant dynamic components of the system. Most of the recordings that were examined exhibited a PDM with frequency response characteristics similar to the PDM1 shown in Fig. 4. This implies that changes in the sign and the level of the input signal play an important role in spike triggering. Under resting conditions, beta-band (13-30 Hz) activity in patients with Parkinson's disease is prominent in the STN. In cases where the LFP signal exhibited significant power in beta-band frequencies, PDMs with low and high frequency characteristics were observed (Fig. 11).

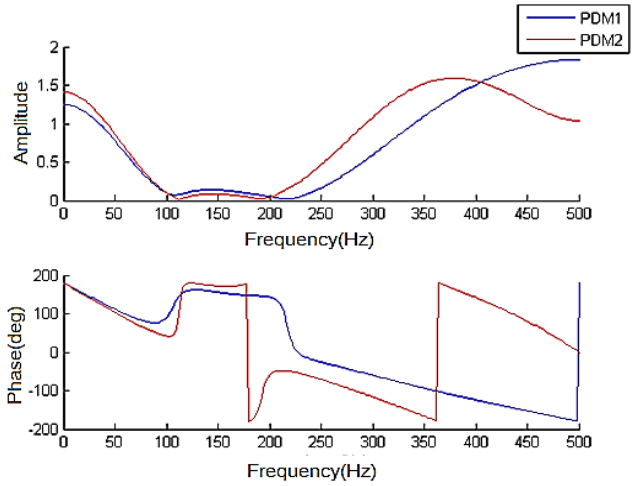

Figure 11: PDMs from a recording with its LFP signal exhibiting significant power in the beta-band (13-30 Hz)

In most of cases, both second-order Volterra and PDM models were able to predict the presence of spike events with good accuracy (MCC values for the testing set between 0.6 and 0.89). In recordings with non-separable multi-unit activity, second-order Volterra models exhibited a tendency to overfit the data. On the contrary, first-order and PDM models seemed to capture the timing of the actual spike trains better. Still, the prediction accuracy was lower compared to single-unit activity predictions.

The results presented in this paper demonstrate the ability to infer spike trains from the LFP of Parkinson's disease patients using nonlinear dynamic modeling. Our findings suggest that LFPs carry information that is predictive of the timing of single-unit spikes. Moreover, the PDM methodology is able to capture the most prominent dynamic characteristics of the system associated with spike triggering in the STN. Our next step is to examine thoroughly the contribution of different frequency bands (especially the low and beta-band frequencies) of the LFP signal to the spike triggering mechanism of the Parkinsonian STN.

References

[1] J.A. Obeso, C.W. Olanow, M.C. Rodriguez-Oroz, P. Krack, R. Kumar, and A.E. Lang, "Deep-brain stimulation of the subthalamic nucleus or the pars interna of the globus pallidus in Parkinson's disease," N. Engl. J. Med., vol. 345, pp. 956–963, 2001.

[2] A.D. Legatt, J. Arezzo, H.G. Vaughan, "Averaged multiple unit activity as an estimate of phasic changes in local neuronal activity: effects of volume-conducted potentials," J. Neurosci. Methods., vol. 2, 1980, pp. 203-217.

[3] U. Mitzdorf, "Properties of the evoked-potential generators: current source-density analysis of visually evoked-potentials in the cat cortex," Int. J. Neurosci., vol. 33, 1987, pp. 33-59.

[4] A. Kamondi, L. Acsady, X.J. Wang, and G. Buzsaki, " Theta oscillations in somata and dendrites of hippocampal pyramidal cells in vivo: activity-dependent phase-precession of action potentials," Hippocampus, vol. 8, pp. 244–261, 1998.

[5] K.P. Michmizos, D.E. Sakas, K.S. Nikita, «An in-silico model of an STN neuron that uses the LFPs to predict the spikes", Consciousness and its Measures, Limassol, Cyprus, November 29- December 1, 2009.

[6] K.P. Michmizos, K.S. Nikita, "Can We Infer Subthalamic Nucleus Spike Trains from Intranuclear Local Field Potentials?," EMBC '10, Buenos Aires, Argentina, September 2010.

[7] K.P. Michmizos, D.E. Sakas and K.S. Nikita, "Prediction of the timing and the rhythm of the parkinsonian subthalamic nucleus neural spikes using the local field potentials," IEEE Transactions of Information Technology in Biomedicine, 2011.

[8] K.P. Michmizos, D.E. Sakas and K.S. Nikita, "Towards relating the subthalamic nucleus spiking activity with the local field potentials acquired intranuclearly," IOP Measurement Science and Technology, 2011.

[9] G.D. Mitsis, A.S. French, U. Hoger, S. Courellis and V Z. Marmarelis. "Principal Dynamic Mode Analysis of Action Potential Firing in a Spider Mechanoreceptor," Biol. Cybern. 96: 113-127, 2007.

[10] G.D. Mitsis. "The Volterra-Wiener approach in neuronal modeling," Conf Proc IEEE Eng Med Biol Soc. 2011.

[11] G.D. Mitsis and V.Z. Marmarelis. "Modeling of Nonlinear Systems with Fast and Slow Dynamics. I. Methodology," Ann. Biomed. Eng. 30: 272-281, 2002.

[12] V.Z. Marmarelis, "Nonlinear Dynamic Modeling of Physiological Systems" Piscataway, NJ: Wiley-Interscience & IEEE Press, 2004.

[13] V. Z. Marmarelis, "Identification of nonlinear biological systems using laguerre expansions of kernels," Annals of Biomedical Engineering, vol. 21, pp. 573–589, 1993.

[14] V. Z. Marmarelis, "Modeling methology for nonlinear physiological systems," Annals of Biomedical Engineering, vol. 25, pp. 239–251, 1997.

[15] R.Q. Quiroga, Z. Nadasdy, Y. Ben-Shaul. "Unsupervised spike detection and sorting with wavelets and superparamagnetic clustering," Neural Comput. 16(8):1661-87, 2004.

[16] M. Riedmiller, "Rprop - Description and Implementation Details," Technical Report, University of Karlsruhe, 1994.